On Reciprocity Measurements in an Annular Duct

Abstract

This document addresses the development of an experimental technique designed to assess the dipole acoustic transfer function in an annular duct with rigid walls. Preliminary results of this method are presented in order to determine its effectiveness and discover if this same technique could be useful in assessing the dipole acoustic transfer function for different geometries. A detailed knowledge of this transfer function will be useful in future experiments relating to ducted propulsion systems and the propagation of rotor noise into the far field. The method developed utilizes the principal of acoustic reciprocity to calculate the dipole acoustic transfer function, or Green's function, without requiring the use of an idealized dipole source. The measured Green's function relates a unit strength of the dipole source to the sound pressure that propagates into the far field. A probe consisting of two microphones placed a known distance apart was used to assess the acoustic dipole transfer function in the annular duct. The transfer function was calculated for several radial locations of the microphone probe, allowing for the measurement and detection of duct modes and other acoustic phenomena.

Mike Lisman

Undergraduate Thesis

Submitted: April 29, 2005

Table of Contents

1.0 Introduction

The first portion of this document discusses the experimental techniques used to calculate the dipole acoustic transfer function for an annular duct. These techniques include the development of a probe consisting of two phase-mismatched microphones that were designed for use in small hearing aids. The second portion of the document contains the results obtained for the transfer function of an annular duct using the aforementioned microphone probe.

The annular geometry is of particular importance for the evaluation of rotor noise sources located inside ducted propulsion systems. The Green's function for an annular duct relates the acoustic source strength to the sound pressure at an observation point in the far field. The objective of the present investigation was to experimentally determine the transfer functions relating this source strength to the sound pressure observed in the far field.

There are many idealized sources of sound, each having its own unique pressure field. The point monopole is a point source which radiates sound uniformly in all directions. Because it radiates sound uniformly in all directions, an infinitely small, pulsating sphere can be idealized as a monopole. The dipole is composed of two point monopoles of equal strength that have a phase difference of π radians. It produces no net volume displacement but does apply a force to the fluid. The compact dipole is formed when the distance between these two point monopoles is much less than its acoustic wavelength. An oscillating sphere exerts only a force on the fluid and does not produce a net displacement, and thus results in a far field pressure identical to the point dipole. A quadrupole is an arrangement of four monopoles that produces neither a net volume displacement nor a net force on a fluid.

A waveguide is a duct or pipe which affects the direction and manner in which sound travels. The manner of this sound travel through the waveguide is frequency dependent, and can give rise to organ pipe duct modes or combinations of both organ pipe modes and higher order duct modes at frequencies above the cut-on frequency. This cut-on frequency is a characteristic of the duct diameter.

The free-space Green's function is used to determine the pressure at a given point produced by a unit strength of a point monopole. Application of the principle of acoustic reciprocity permits calculation of the dipole acoustic transfer function, or Green's function, by interchanging the locations of the source and observation point. A Green's function is used to solve a differential equation that is subject to particular boundary conditions. The Green's function relates the sound pressure at a given point to the source location and is a solution to the wave equation. The Helmholtz Equation which governs linear acoustics is given by

$$\nabla^2 P + \left(\frac{\omega}{c}\right)^2 P = 0 \,. \tag{1}$$

Green's function is a solution to the equation,

$$\nabla^2 G(\omega) + \left(\frac{\omega}{c}\right)^2 G(\omega) = \delta(\vec{x}, \vec{x}_0) \,. \tag{2}$$

An important property of the Green's function is that it is symmetric. That is:

$$G(\vec{x}, \vec{x}_0, \omega) = G(\vec{x}_0, \vec{x}, \omega) \,. \tag{3}$$

This property indicates that the source locations and observation point in the far field may be interchanged without affecting the Green's Function. The principle of acoustic reciprocity expressed explicitly in Equation (3) can be utilized with a known source in the far field and a

microphone pair placed at known locations in the duct. The pressure difference between the two microphones can be determined in order to calculate the dipole acoustic transfer function for the annular duct.

2.0 Experimental Technique

The most direct method of calculating the dipole acoustic transfer function for an annular duct involves placing an idealized dipole source in the duct and conducting sound pressure measurements in the far field. However, this experimental method was not utilized because a perfect dipole source cannot presently be obtained. Use of any source that approximates an acoustic dipole would introduce a large amount of error and decrease the accuracy of the experiment. An alternative and more accurate method was developed through application of the principle of acoustic reciprocity.

A probe consisting of two microphones was constructed in order to measure a local pressure gradient. This pressure gradient is necessary for the calculation of the dipole acoustic transfer function. A pair of phase-matched microphones could not be used due the physical limitations of the duct size and the need to place the microphones sufficiently close to calculate the dipole acoustic transfer function. Two significantly smaller hearing aid microphones were placed 2.2 cm apart at one end of a probe which could be extended into a duct with the use of an aluminum sting. This reciprocity probe enables the microphones to be rotated through a maximum angle of 180° and allows for the calculation of the dipole acoustic transfer function, as detailed below. A picture of the probe is shown in Figure 1.

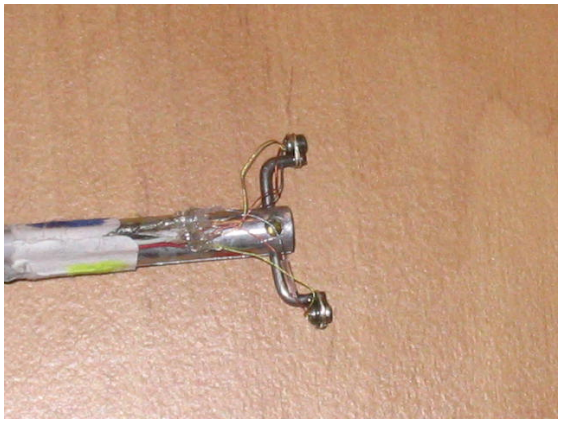

Figure 1: Probe at 0° Angle

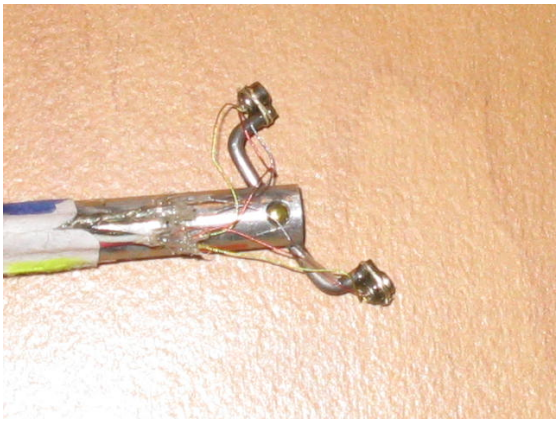

Figure 2: Probe at 45° Angle

The dipole acoustic transfer function was assessed by placing the probe at angles of 45˚ and -45˚ while in the duct. Figure 2 shows the probe at an angle of 45˚. A schematic of the experimental setup is shown in Figure 3. The reciprocity probe was placed in the annular duct such that the microphones were positioned at the propeller location, shown in blue in the figure. An omnisource speaker was used to approximate a point source and generated spherical waves that propagated towards the duct inlet. Because the omnisource does not radiate pressure uniformly at all frequencies, a reference microphone was positioned outside the inlet in order to measure the radiated acoustic pressure.

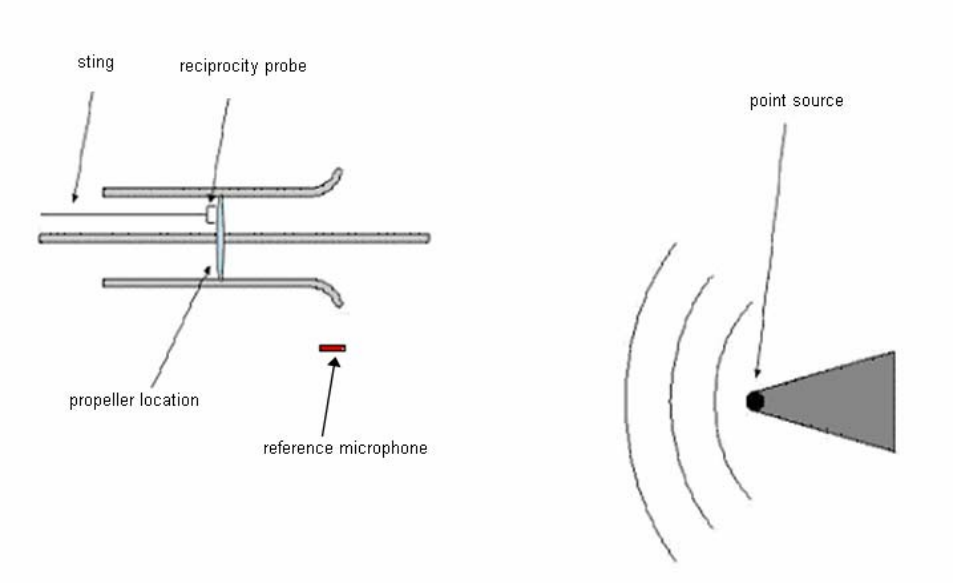

Figure 3: Experimental Setup

The dipole acoustic transfer function can be calculated as follows:

$$\frac{P_{rad}}{F_{dipole}} = \frac{1}{4\pi V x r}\sqrt{\frac{G_{VP}}{G_{PP}}} \qquad (4)$$

where the ratio P_{rad} / F_{dipole} is the dipole acoustic transfer function, Δx is the distance between the two probe microphones, r is the distance from the point source to the reference microphone, $G_{\Delta P}$ is the auto spectral density of the pressure difference between the two probe microphones, and G_{PP} is the auto spectral density of the pressure measured by the reference microphone.

Placement of the microphone probe at angles of 45˚ and -45˚ in the duct allows for an estimation of the dipole acoustic transfer function in both the axial and transverse directions, as shown in Figure 4.

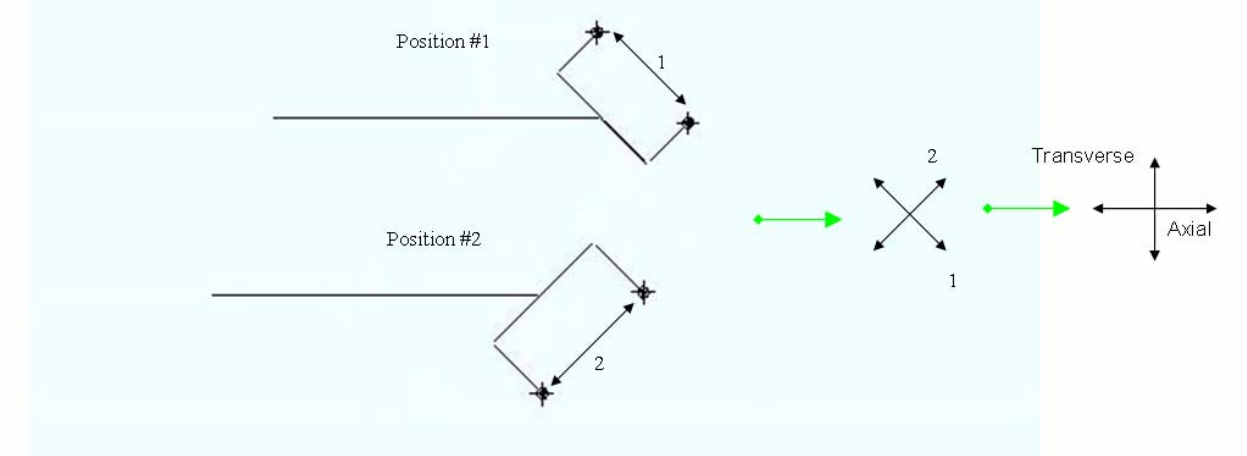

Figure 4: Obtaining Axial and Transverse Dipole acoustic transfer functions

The phase-mismatch of the two probe microphones was accounted for during the calibration. Early in the microphone calibration stages, it was discovered that this phase difference was of sufficient magnitude to introduce a sufficiently large amount of error. Moreover, it was also found that the phase difference exhibited frequency dependence.

Calibration of the two smaller hearing aid microphones located on the probe required the use of a single Bruel & Kjaer (B&K) microphone that was used as a reference. Placement of the microphone probe at an angle of zero degrees and directly next to the single B&K microphone ensured that within reasonable error limits, both the two hearing aid microphones and the B&K microphone were subject to the same acoustic pressure at a given time.

Initial attempts to conduct the calibration in anechoic space indicated that at higher sound frequencies close to 2000 Hz, reflected waves interfered with the microphone calibration. Theoretically, the placement of the microphone probe at an angle of zero degrees should yield a phase angle which results entirely from the effects of the inherent electrical differences between

the two microphones. As shown in blue in Figure 5, this phase angle exhibited small oscillations over the entire frequency spectrum and a slight departure from the desired phase angle result of zero at lower frequencies. Placement of the probe in a plane wave tube yielded the improved results shown in red in Figure 5, indicating that previous problems encountered in anechoic space were the results of reflected sound waves and not the inherent electrical phase mismatch between the two microphones. The effect of such reflected waves on the measured phase difference between the two microphones is rather drastic. While such reflected waves can roughly double the acoustic pressure resulting in an increase of only 2-3 dB for the measured sound magnitude, their effect on the measured phase angle is much larger and can increase this quantity by as much as a factor of two.

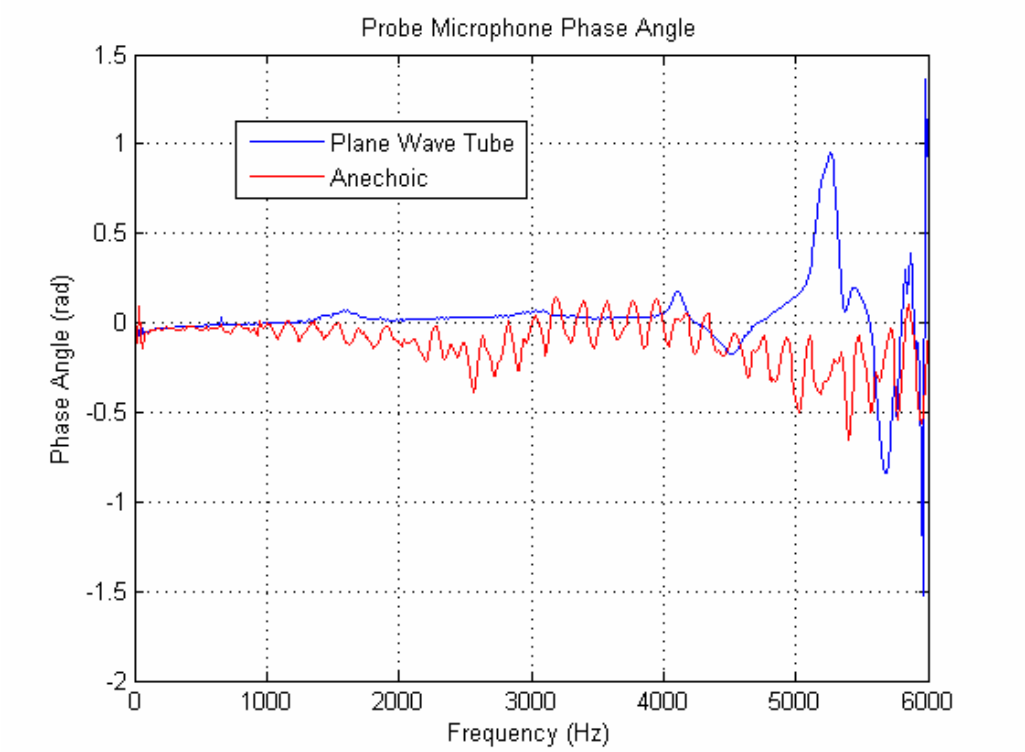

Figure 5: Anechoic vs. Plane Wave Tube Phase Angles for Probe Microphones

Placement of the probe in a plane wave tube ensures that no reflected waves are generated for sound frequencies below the cut-on frequency. Above the cut-on frequency, reflections will

occur off of the walls of the tube, and there are wave phenomena in the duct which can no longer be simply described as planar. A schematic depicting the experimental setup for the plane wave tube calibration is shown in Figure 6.

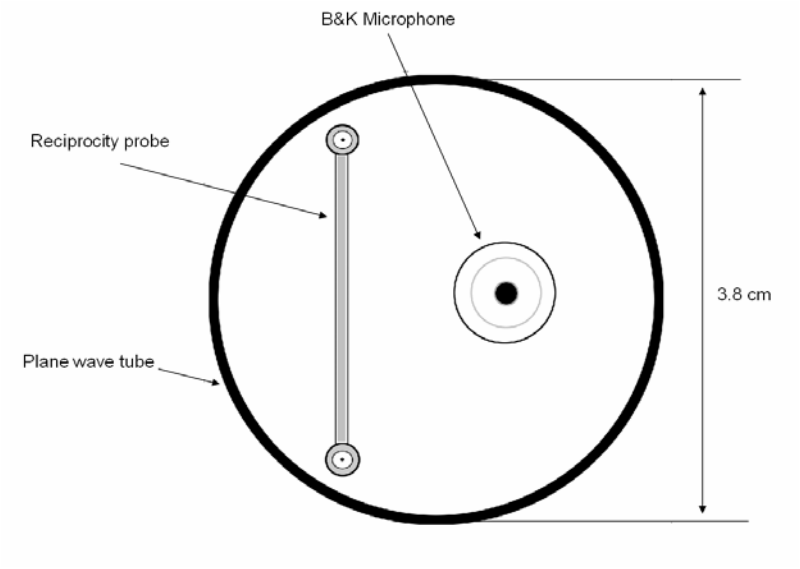

Figure 6: Plane Wave Tube Calibration

Calibration of the two smaller microphones located on the probe allowed for the determination of a transfer function relating the measured microphone voltage to the pressure detected by the microphone. This technique involved placing the B&K microphone as close as possible to the probe microphones and subjecting this combination of three microphones to white noise. Assuming that all three microphones encountered the same acoustic pressure at a given time, the microphone transfer function is defined as:

$$H_1(\omega) = \frac{G_{PV_1}}{G_{V_1V_1}} \tag{5}$$

where G_{PV_1} is the cross spectral density of the pressure measured by the B&K microphone with the voltage measured by one of the probe microphones and $G_{V_1V_1}$ is the auto spectral density of the

voltage time series recorded by the probe microphone during the calibration (Bendat, Persol). The respective microphone transfer function and cross spectral density of the pressure measured by the second probe microphone with the corresponding voltage ($H_2(\omega)$ and $G_{P_2V_2}$) may be determined in a manner analogous to that described for the first probe microphone and as detailed in the preceding equation. The transfer function of each microphone allows for the determination of the squared value of the acoustic pressure measured by each of the probe microphones as a function of sound frequency according to the equation

$$G_{P_1P_1} = \left|H_1(\omega)\right|^2 G_{V_1V_1} . \tag{6}$$

As noted, determination of the dipole acoustic transfer function requires calculation of the pressure difference between the two probe microphones. Equation (6) allows for the computation of both $G_{P_1P_1}$ and $G_{P_2P_2}$. This pressure difference can be obtained by:

$$G_{VP} = G_{P_1P_1} + G_{P_2P_2} - 2(G_{P_1P_2})_{real} \tag{7}$$

where G_{VP} is the square of the pressure difference between the two probe microphones as a function of frequency and $(G_{P_1P_2})_{real}$ is the real component of the cross spectral density of the two probe microphones. The quantity $G_{P_1P_2}$ can be obtained from the following analysis involving the transfer function H(f) and the two quantities the function relates, P(f) and V(f):

$$P(f) = H(f)V(f) \tag{8}$$

The auto spectral density of the pressure can be expressed as

$$G_{P_1P_2}(f) = E\left[P_1(f)P_2^*(f)\right] , \tag{9}$$

where "E" denotes the expected value. Substitution of Equation (8) into Equation (9) yields

$$G_{P_1P_2}(f) = E\left[H_1(f)V_1(f)\cdot H_2^*(f)V_2^*(f)\right] . \tag{10}$$

Because the transfer functions for the two probe microphones are determined in the calibration and are thus constant, Equation (10) becomes

$$G_{P_1P_2}(f) = H_1(f)H_2^*(f) \times E\left[V_1(f) \cdot V_2^*(f)\right]. \qquad (11)$$

Utilizing the same relationship expressed in Equation (9), the above relationship can be expressed as

$$G_{P_1P_2}(f) = H_1(f)H_2^*(f)G_{V_1V_2}. \qquad (12)$$

3.0 Preliminary Duct Transfer Function Results

The dipole acoustic transfer function was assessed for two different locations of the point source. The probe microphone transfer functions were evaluated by averaging the results of four different calibrations conducted in the plane wave tube. A schematic of the annular duct cross section is shown in Figure 7. As shown in the figure, the duct contains a circular center body of 5.72 cm diameter that extends throughout its entire length. The two different cases studied for separate locations of the point source are shown in Figures 8 and 9. As discussed in Section 1.0, the microphone probe was placed at the axial location in the duct where the propeller will be located in future experiments. This placement allows for the calculation of the appropriate transfer function.

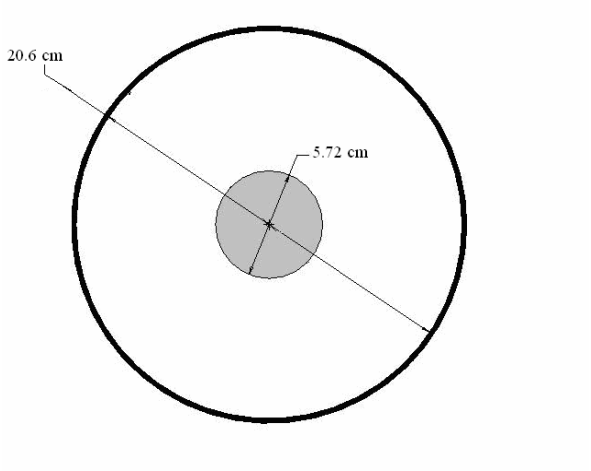

Figure 7: Duct Cross Section with Center Body

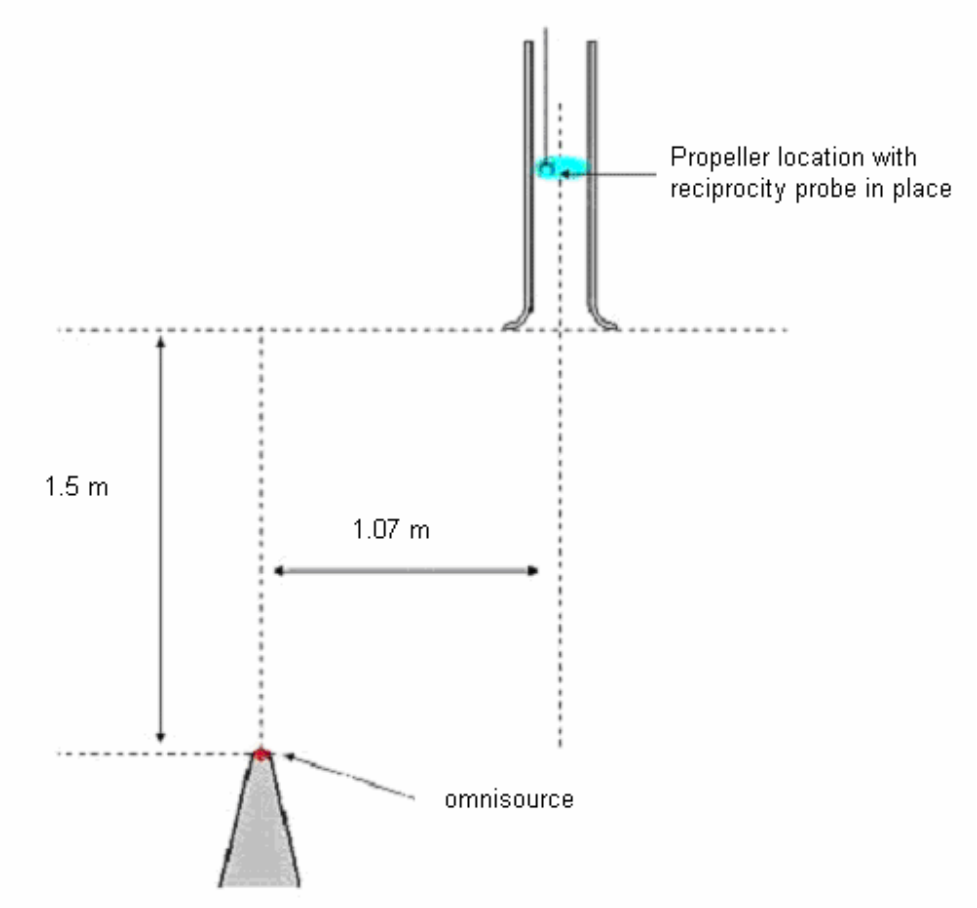

Figure 8: Point Source Position I

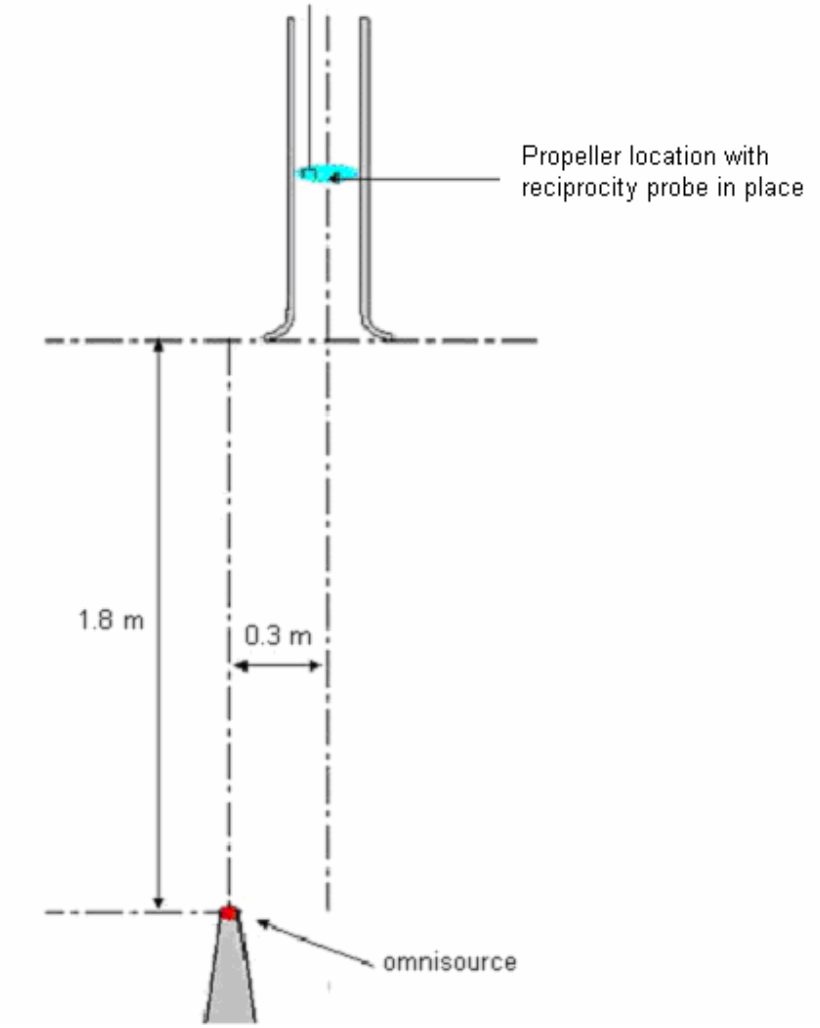

Figure 9: Point Source Position II

The probe was placed at several different radial locations in order to assess the dipole acoustic transfer function in different regions of the duct. The transfer functions were obtained for several different radial locations and were found to exhibit many key similarities. First, the acoustic duct modes were found to have a large effect on the transfer functions. The first mode for the 20.6 cm diameter duct was found to occur at 152.4 Hz, as shown in Figure 10.

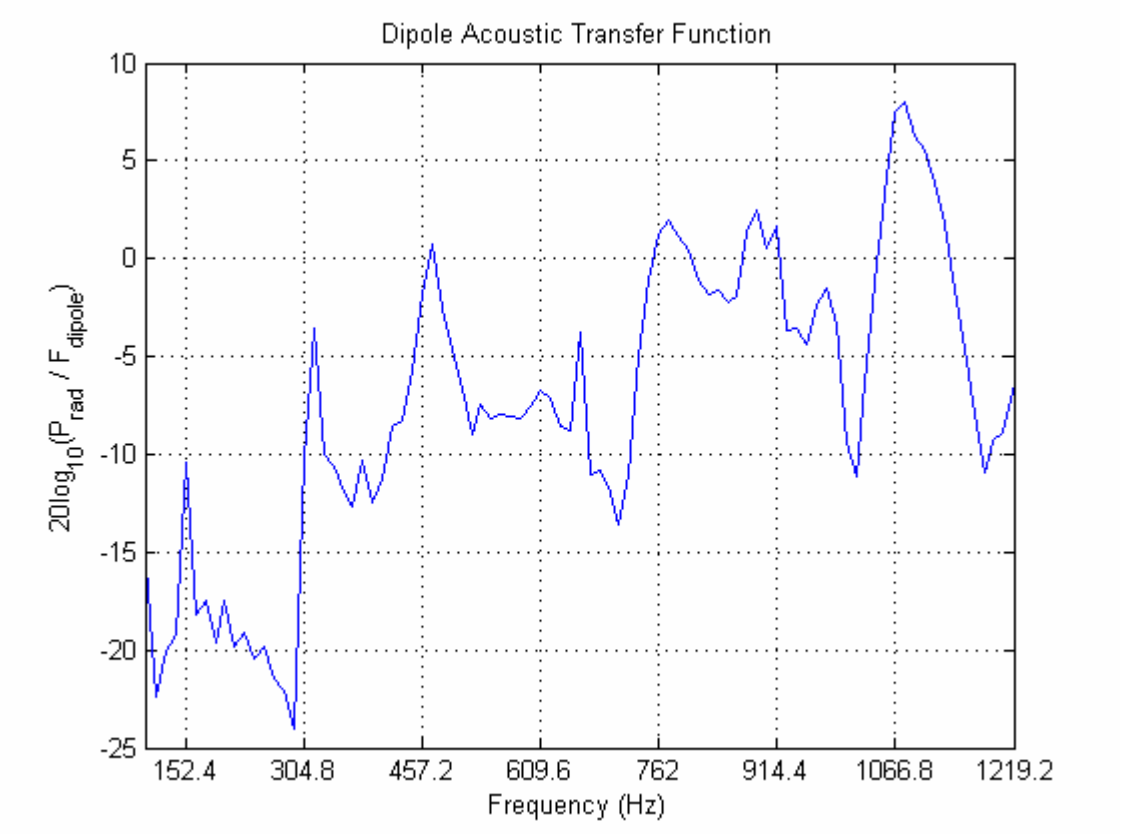

Figure 10: "Organ Pipe" Duct Modes at Lower Frequencies

As shown in Figure 10, the duct modes occurred at frequencies which were multiples of 152.4 Hz, causing sharp increases in the magnitude of the transfer function at these frequency values. The first several duct modes are clearly visible in the figure.

As discussed earlier, additional duct modes will also be present in the duct at frequencies above the cut-on frequency. These modes exist above the cut-on frequency of ≈ 975 Hz, a characteristic of the duct diameter. As shown in Figure 11, there are additional complexities in the dipole acoustic transfer function above this cut-on frequency.

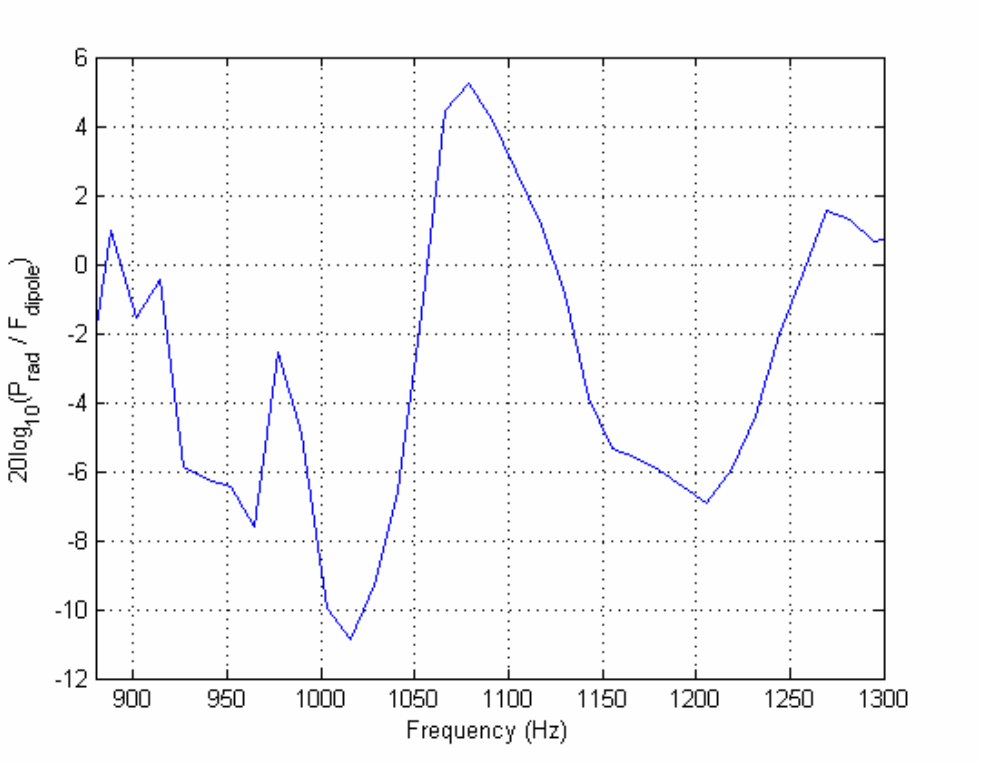

Figure 11: Complexity of the Transfer Function Above the Cut-On Frequency

A decrease in the magnitude of the dipole acoustic transfer function was observed for probe locations placed at successively larger distances from the duct's center, indicating that the magnitude of the transfer function does exhibit some radial dependence. Figures 12 and 13 display this relationship for the lower frequency range and two different radial positions, 3.81 cm and 6.35 cm off of the duct centerline.

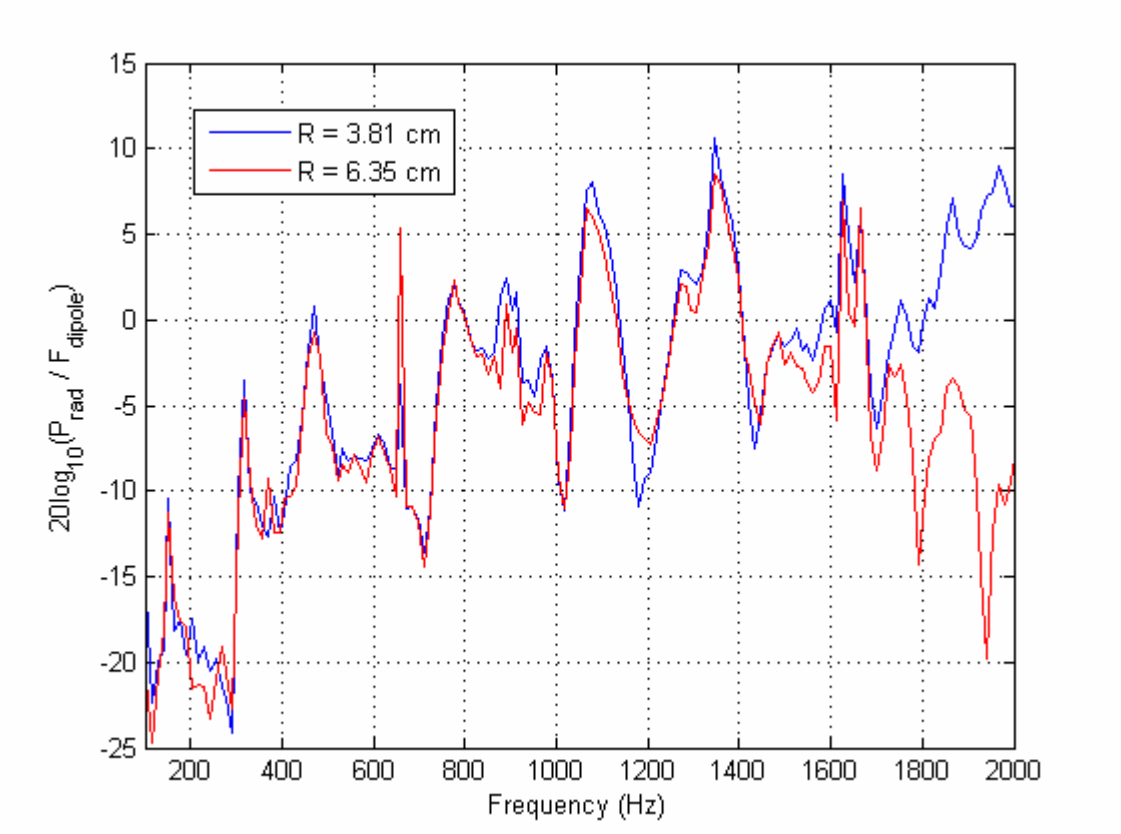

Figure 12: Radial Dependence of Transfer Function

Figure 13 shows only the magnitude of the transfer function at each of the first several duct modes for two different radial positions. As indicated, the strength of the dipole vector decreases for successively larger radii at all frequencies except 660 Hz. At this frequency, there is a very large difference in the magnitudes of the transfer functions that does not follow the trend of decreasing magnitude for larger radii. In both Figures 12 and 13, it is clearly evident that at a frequency of 660 Hz, the magnitude of the transfer function is much larger for a radius of 6.35 cm.

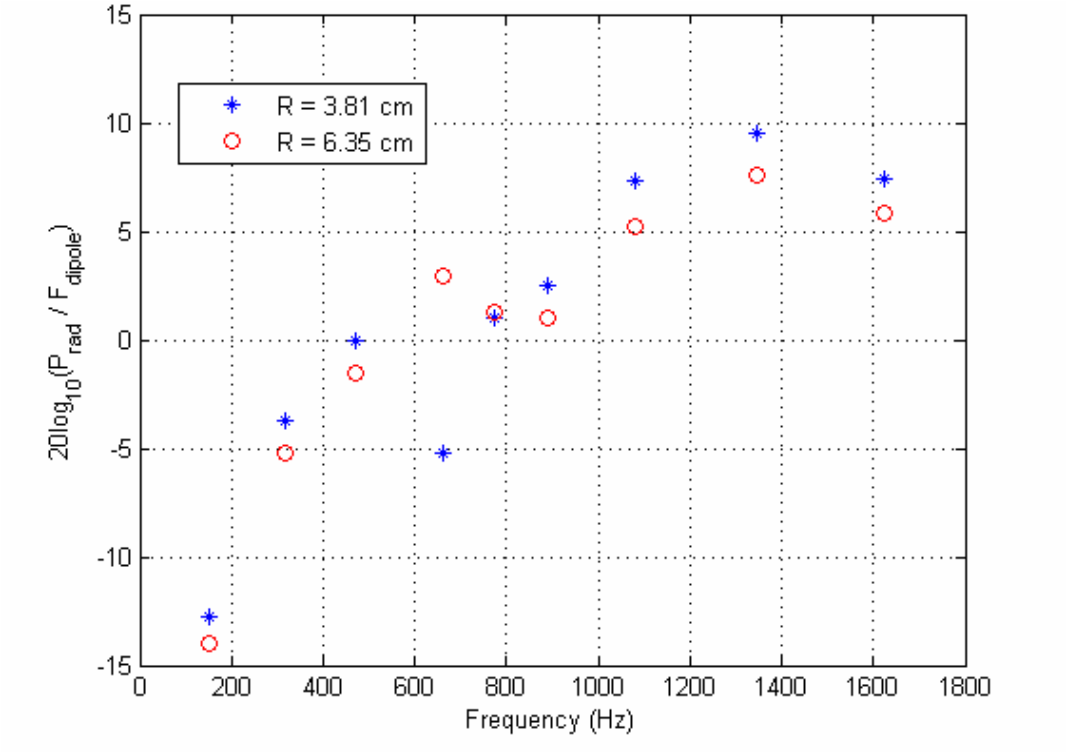

Figure 13: Magnitude of the Transfer Function at the first nine duct modes for two different radial positions

The location of the point source was also found to have a slight impact on the measured magnitude of the transfer function. The two omnisource positions detailed in Figures 8 and 9 produced duct modes at approximately the same frequencies. However, the magnitude of the transfer function was found to be greater for the second point source position, shown in Figure 9. This result is depicted below in Figure 14, which displays the transfer function at the same radial location for the two different positions of the point source. As shown, the location of the point source has little effect on the frequencies at which the duct modes were found to occur. However, at frequencies above 1000 Hz, slight variations do become evident. Although the magnitude of the transfer function still follows the same trend for both point source positions, the duct modes appear to occur both over a varying frequency range and at slightly different frequency values.

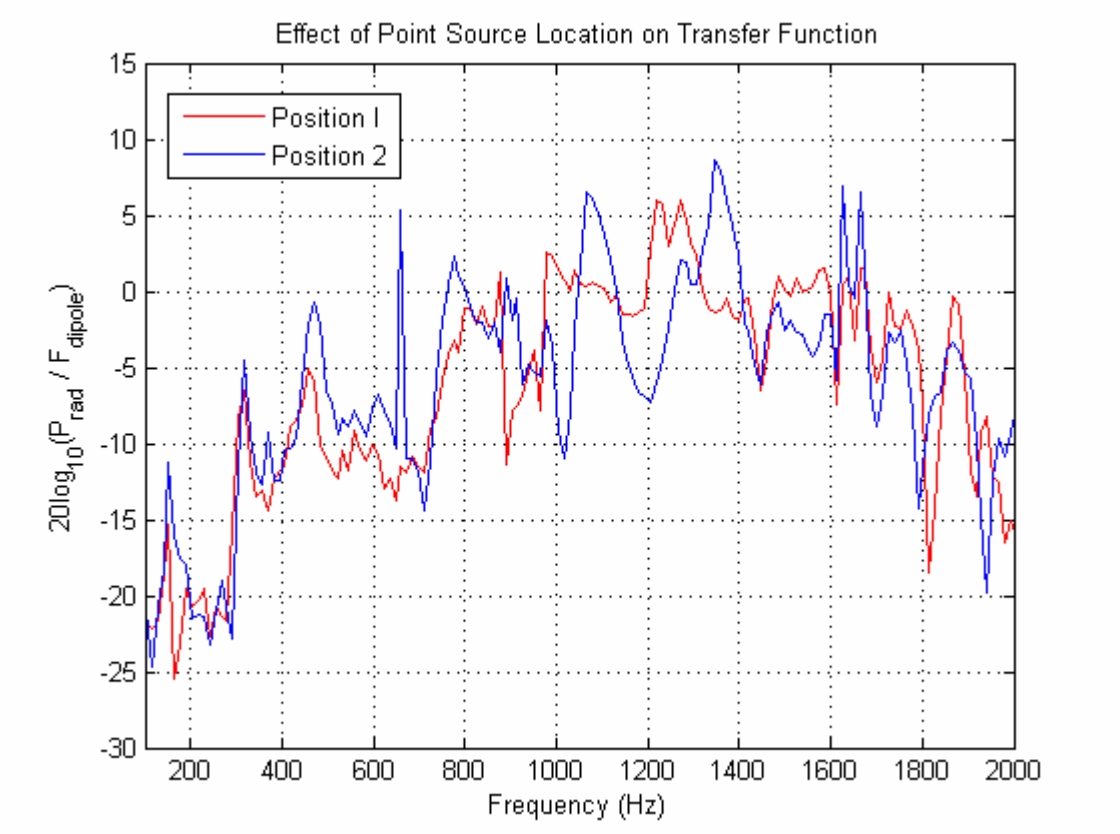

Figure 14: Effect of Point Source Location on the Transfer Function

The results of the reciprocity measurements conducted using the probe were also compared with other acoustic data obtained for the annular duct. Previously conducted experiments have involved the sampling of sound pressure in the far field when a propeller was placed in the annular duct and operated at several speeds. An average transfer function was calculated for the annular duct using the individual transfer functions obtained at each of ten radial positions. This average transfer function is shown in Figure 15 and compared with the results of the experiments conducted using the propeller. The figure indicates that the results obtained using the different experimental techniques are in close agreement with one another, particularly for the lower frequencies below 700 Hz.

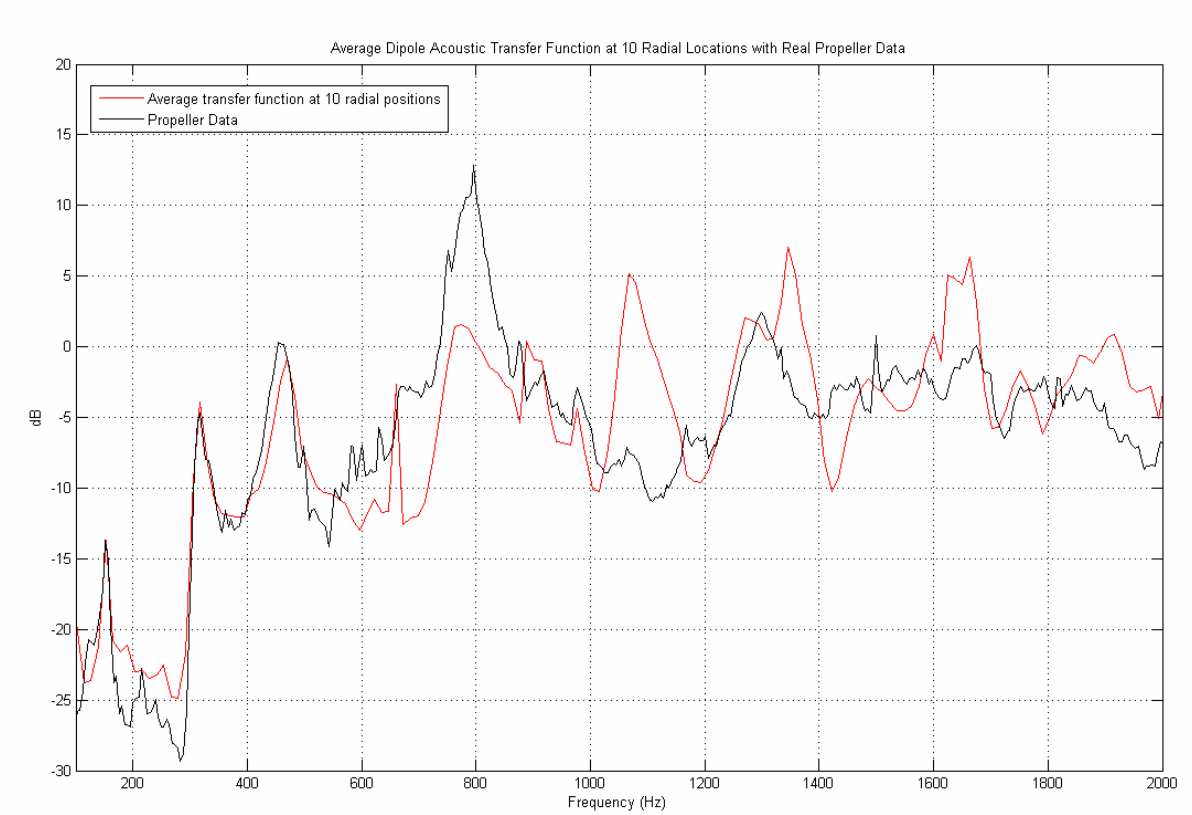

Figure 15: Comparison of Average Transfer Function with Results Obtained Using Propeller

4.0 Summary and Conclusions

The microphone probe designed is effective in measuring the strength of the dipole vector in the annular duct. The computational methods used in analyzing the duct provide a convenient method of accounting for the inherent phase difference between the two microphones located on the probe. The experimental technique detailed in this document could be applied to a variety of different geometries and be used to accurately assess the strength of the dipole vector for each. The dipole transfer function obtained for the annular duct indicates the presence of several duct modes. The strength of the dipole vector was found to exhibit some radial dependence and

weakened slightly for larger distances from the duct's center. Assessment of the dipole acoustic transfer function for two different locations of the point source indicated that the frequencies at which the duct modes occur were generally unaffected by this change in point source position. However, the strength of the dipole vector was found to be slightly greater for point source position II detailed in Figure 9. The average dipole acoustic transfer function calculated using reciprocity and the results of far field pressure measurements conducted in the same annular duct with an operational propeller are in close agreement with one another, particularly at lower sound frequencies.

5.0 References

Fahey, Frank. *Foundations of Engineering Acoustics*. London, UK: Academic Press, 2001.

Bendat, JS & Persol, AG. *Random Data - Analysis and Measurement Procedures*, 2nd Edition. New York: John Wiley & Sons, 1986.